





Critical Evaluation of Green Synthesized Silver Nanoparticles-Kaempferol for Antibacterial Activity Against Methicillin-Resistant *Staphylococcus aureus*

Ariff Haikal Hairil Anuar ¹, Siti Aisyah Abd Ghafar ¹, Rohazila Mohamad Hanafiah ¹,
Vuanghao Lim ², Nur Farah Atiqah Mohd Pazli¹

¹Department of Basic Sciences, Faculty of Dentistry, Universiti Sains Islam Malaysia, Kuala Lumpur, 55100, Malaysia; ²Integrative Medicine Cluster, Advanced Medical and Dental Institute, Universiti Sains Malaysia, Kepala Batas, Penang, 13200, Malaysia

Correspondence: Siti Aisyah Abd Ghafar, Department of Basic Sciences, Faculty of Dentistry, Universiti Sains Islam Malaysia, Level 18, Tower B, Persiaran MPAJ, Jalan Pandan Utama, Kuala Lumpur, 55100, Malaysia, Tel +60389471157, Fax +60389472566, Email aisyahghafar@usim.edu.my

Introduction: This study aimed to characterize silver nanoparticles-kaempferol (AgNP-K) and its antibacterial activities against methicillin-resistant *Staphylococcus aureus* (MRSA). Green synthesis method was used to synthesize AgNP-K under the influence of temperature and different ratios of silver nitrate (AgNO₃ and kaempferol).

Methods: AgNP-K 1:1 was synthesized with 1 mM kaempferol, whereas AgNP-K 1:2 with 2 mM kaempferol. The characterization of AgNP-K 1:1 and AgNP-K 1:2 was performed using UV-visible spectroscopy (UV-Vis), Zetasizer, transmission electron microscopy (TEM), scanning electron microscopy-dispersive X-ray spectrometer (SEM-EDX), X-ray diffraction (XRD), and Fourier transform infrared (FTIR) spectroscopy. The antibacterial activities of five samples (AgNP-K 1:1, AgNP-K 1:2, commercial AgNPs, kaempferol, and vancomycin) at different concentrations (1.25, 2.5, 5, and 10 mg/mL) against MRSA were determined via disc diffusion assay (DDA), minimum inhibitory concentration (MIC), minimum bactericidal concentration (MBC) assay, and time-kill assay.

Results: The presence of a dark brown colour in the solution indicated the formation of AgNP-K. The UV-visible absorption spectrum of the synthesized AgNP-K exhibited a broad peak at 447 nm. TEM, Zetasizer, and SEM-EDX results showed that the morphology and size of AgNP-K were nearly spherical in shape with 16.963 ± 6.0465 nm in size. XRD analysis confirmed that AgNP-K had a crystalline phase structure, while FTIR showed the absence of (-OH) group, indicating that kaempferol was successfully incorporated with silver. In DDA analysis, AgNP-K showed the largest inhibition zone (16.67 ± 1.19 mm) against MRSA as compared to kaempferol and commercial AgNPs. The MIC and MBC values for AgNP-K against MRSA were 1.25 and 2.50 mg/mL, respectively. The time-kill assay results showed that AgNP-K displayed bacteriostatic activity against MRSA. AgNP-K exhibited better antibacterial activity against MRSA when compared to commercial AgNPs or kaempferol alone.

Keywords: nanoparticles, silver nanoparticles, green synthesis, kaempferol, methicillin-resistant *Staphylococcus aureus*

Introduction

Methicillin-resistant *Staphylococcus aureus*, also known as MRSA, is a Gram-positive bacterium belonging to the family of *Staphylococcaceae*. MRSA is nowadays a worldwide public health threat due to the resistance to current antibiotics such as linezolid, quinupristin/dalfopristin, daptomycin, and telavancin.^{1,2} MRSA is a subspecies strain of *S. aureus*, categorized under superbugs which developed resistance towards β -lactam antibiotics such as methicillin, oxacillin, and cephalosporins.^{3,4} MRSA tends to develop in waves of infection, which are typically identified by the repeated emergence of dominant strains.¹ This, in turn, results in limited choices of treatment for MRSA infections. Poor infection control procedures, along with continuous unselective antibiotic contact between humans and animals, have caused massive problems in MRSA acquisition and transmission. According to the Centers for Disease Control and Prevention (CDC), MRSA infections often cause skin infections and the worst infections may occur, such as pneumonia (lung infections) and sepsis. Thus, new antibiotic-based nanotechnologies are required to prevent MRSA infections.

Nanotechnology has been widely studied in the past decades, offering boundless potential in a wide variety of applications, such as chemistry, physics, biology, engineering, and health sciences.⁵ This has triggered high interest among researchers in this field. Gold, silver, and metal are among the most popular nanoparticles (NPs) that have been studied. AgNPs synthesis has gained popularity among researchers, and numerous investigations have been conducted using diverse chemical, physical, and biological (green) approaches.⁶ The most common methods for synthesizing AgNPs are chemical and green techniques. The chemical synthesis method uses several chemicals to produce AgNPs. However, green synthesis is a direct method that uses plants to produce AgNPs; thus, green synthesis is more feasible than chemical synthesis. Common chemicals used to synthesize AgNPs are sodium borohydride, hydrazine, and ethylene glycol.⁵ The green synthesis technique is the most popular method for synthesizing nanoparticles. This technique uses plant-based reagents as reducing and capping agents because of the bioactive compounds found in plants such as phenolic compounds.^{5,7,8} The effectiveness of AgNPs can be proven by using water (H₂O) as a solvent; therefore, there will be no other chemical present that influences the results. Previous studies have reported that AgNPs synthesized using plant extracts such as *Aegle marmelos*, red seaweed *Spyridia filamentosa*, *Mangifera indica*, vegetable waste, and *Cocos nucifera* exhibited significant antibacterial activity against *Staphylococcus aureus*, *Escherichia coli*, and other bacteria.^{9–13} Kaempferol, a flavonoid derived from plant sources, is a bioactive compound that reduces silver ions (Ag⁺) to silver (Ag⁰). Kaempferol possesses antibacterial activity but is limited by the characteristics of kaempferol.⁶ Kaempferol consists of aromatic hydrocarbons that are mainly nonpolar. Nonpolar compounds have a weak attractive force between the particles, which makes them harder to dissolve in water; thus, a homogenous solution cannot be achieved. This was strongly proven by the chemical structure of kaempferol-containing diphenylpropane, which is responsible for its low water solubility properties or hydrophobicity.⁶ A previous study reported that kaempferol, incorporated with AgNPs synthesized using polyvinyl pyrrolidone (PVP) solution and ethanol as their dissolving solvents, exhibited antibacterial activity against *S. aureus* and *E. coli*.⁵ To date, there is no AgNP-K that has been synthesized via the green synthesis method with observation of its antibacterial activity against MRSA. This study used only ultrapure water with the assistance of heat and time. Hence, this study aimed to evaluate the antibacterial activity of green synthesized AgNP-K against methicillin-resistant *Staphylococcus aureus* (MRSA).

Materials and Methods

Green Synthesis of Silver Nanoparticles-Kaempferol (AgNP-K)

In this study, the green synthesis method was applied with some modifications from a previous study with the usage of different concentrations of kaempferol (Indofine, US) (1.0 mMol and 2.0 mMol) in 1 Litre of ultrapure water (H₂O).^{5,14} Briefly, 1.0 mMol of kaempferol was added drop by drop into continuously stirred silver nitrate (AgNO₃) (1.0 mMol). The mixture was heated in an oven at 60 °C for 168 h. Colour changes from clear to brown were observed. The sample was then freeze-dried (Martin Christ Alpha 1–2 LDplus) to obtain AgNP-K powder. The same procedure was repeated with 2.0 mMol of kaempferol. AgNP-K (1.0 mMol of kaempferol) was labelled as AgNP-K (1:1), while AgNP-K (2.0 mMol of kaempferol) was labelled as AgNP-K (1:2).

Characterization of AgNP-K

The formation of AgNP-K during the reduction of (Ag⁺ - Ag⁰) was monitored using UV–visible spectroscopy (UV-Vis). UV–Vis was used to observe the formation of AgNP-K during the synthesis process every 24 h. This was measured from the absorbance peak of AgNP-K in the wavelength range 300–900 nm using Spectramax ID3. Approximately 150 µL of AgNP-K was aliquoted into 96 well plates. The absorbance parameter was set from 300 to 900 nm. The absorbance peak for silver nanoparticles is usually in the range–390–530 nm.^{5,14}

The samples were diluted with ultrapure water (H₂O) to measure the average size, zeta potential, and polydispersity index (PDI) using a Zetasizer analyser (Malvern Zetasizer Nano ZS; Nano-ZS90, Malvern, UK). The samples were diluted, and tested until the smallest size of AgNP-K was obtained. Parameters such as the refractive index of water (1.330), viscosity (0.8872 cP), and temperature (25 °C) were set before the analysis.

Meanwhile, a transmission electron microscope (TEM) was used to determine the shapes, sizes, and morphologies of the NPs through the cross-section of each NPs. The sample was diluted with distilled water and dropped onto a copper grid.

The surface morphology of the NPs was measured by scanning electron microscopy (SEM; Quanta Feg 650 attached to an X-Max 50 energy dispersive X-ray spectrophotometre) (EDX; Oxford Instrument, Abingdon, UK) by placing the sample on the holder and then loading the sample onto the chamber. The images shown were adjusted by increasing the magnification to obtain clearer images of the areas of interest. This analysis also showed the composition percentages of silver contained in AgNP-K from the EDX analysis.

AgNP-K was placed on a glass sample plate holder by flattening and compressing with an X-ray diffraction (XRD) machine (Rigaku Miniflex 600). The holder was mounted onto standard sample stages in the sample chamber. The X-ray wave was beamed, and the scattered intensity was measured using instruments. XRD was used to measure the crystallinity and phases to a certain angular degree. XRD is also used to detect the presence of silver in the compound by referring to the silver database for XRD analysis. This indirectly proves the successful synthesis of AgNP-K by comparison with the standard silver database from the Joint Committee on Powder Diffraction Standard (JCPDS).

Fourier transforms infrared (FTIR) analysis was conducted using Thermo Scientific™ Nicolet™ iS50 FTIR Spectrometer to observe the presence of a functional group in the NPs, such as a hydroxyl group (OH). AgNP-K was placed on a diamond crystal and touched with an ATR touch-point probe.

Antibacterial Activities of AgNP-K Against MRSA

Disc Diffusion Assay (DDA)

The disc diffusion method, also known as the Kirby-Bauer disc diffusion method, was used to determine inhibition zones of AgNP-K against MRSA.^{15,16} MRSA (ATCC number: 33,591) was cultured in brain heart infusion (BHI) broth and incubated overnight at 37 °C. Approximately 0.5 McFarland turbidity standard for MRSA bacteria was used for this analysis. A sterilized cotton swab was used to spread the diluted MRSA (0.5 McFarland) on BHI agar before the application of 5×6 mm paper discs (Whatman No. 1) impregnated with 10 µL of samples (AgNP-K 1:1, AgNP-K 1:2, commercial AgNPs, and kaempferol) at concentrations between 10 mg/mL and 1.25 mg/mL. Sterilized water was used as a negative control and vancomycin (30 U) was used as a positive control.¹⁷ The zones of inhibition were determined from the diameter of the inhibition zone around the disk after incubating the agar plates at 37 °C for 24 h.

Minimum Inhibitory Concentration and Minimum Bactericidal Concentration (MIC and MBC)

Minimum inhibitory concentration (MIC) and minimum bactericidal concentration (MBC) were determined using the two-fold serial dilution method described in a previous study.¹⁸ MIC was done in a sterile 96-well plate. Diluted 0.5 McFarland test bacteria (100 µL) were added to each well of a plate containing diluted samples (AgNP-K 1:1, AgNP-K 1:2, commercial AgNPs, and kaempferol) in sterile BHI broth to a final volume of 100 µL/well. Ultrapure water was used as the negative control and vancomycin 10 mg/mL was used as the positive control. The plates were then incubated at 37 °C for 24 h. An aliquot of 10 µL of 3-(4,5-dimethylthiazol-2-yl)-2,5-diphenyl tetrazolium bromide (MTT) was added and the colour changed to purple. The result was observed visually, and wells that turned purple indicate bacterial growth.¹⁹ The MIC was determined as the lowest concentration that obstructed visible bacterial growth.

The minimum bactericidal concentration (MBC) was used to determine the lowest concentration that killed MRSA. A total of 10 µL aliquoted from wells that displayed no bacterial growth in MIC wells were cultured on BHI agar and incubated overnight at 37 °C. The MBC values were defined as the lowest concentrations that prevented bacterial growth.

Time-Kill Assay

Time-kill assays of AgNP-K 1:1, AgNP-K 1:2, commercial AgNPs, and kaempferol were performed by referring to the method described in previous studies with modifications.^{7,8,20} MRSA bacteria were grown in BHI broth at 37 °C for 24 h. The turbidity of the bacterial culture was adjusted to 0.5 McFarland standard ($\sim 1.5 \times 10^8$ CFU/mL) in sterile fresh BHI broth. AgNP-K samples with concentrations corresponding to the MIC and MBC values were prepared. An aliquot of 100 µL fresh sterile BHI broth was added to a 96-well plate. Next, 100 µL of treatment was added using the serial dilution technique. After that, MRSA bacteria with the amount of 100 µL was added into the well. Next, 10 µL of the treated sample from the plate was aliquoted and added to 2nd 96 well plate filled with 90 µL of sterile BHI broth to perform 10^1 , 10^2 , 10^3 , and 10^4 dilutions. The dilution factors were determined by streaking on BHI agar [4-hour intervals

(0, 4, 8, 12, 16, 20, and 24 h)]. The agar was then incubated at 37 °C for 24 h. The colonies on each plate were counted and expressed as colony-forming units/mL (CFU/mL).⁸

The killing rate of MRSA was determined by the logarithmic number of CFU/mL (\log_{10} CFU/mL) of bacterial growth versus time.²¹ From the observation, the characteristics of the AgNP-K towards MRSA could be determined whether it was bacteriostatic or bactericidal.

Statistical Analysis

Statistical analyses were performed using the Statistical Package for Social Science (SPSS), and significance was accepted at $p < 0.05$. Data presented were analyzed using ANOVA; values are given as mean \pm SD, and means were separated using Tukey's HSD post hoc analysis.

Results

Biosynthesis of Silver Nanoparticles-Kaempferol (AgNP-K)

In this study, the green synthesis method was applied using different concentrations of kaempferol (1.0 mMol and 2.0 mMol) at 60 °C of heat applied for 168 h. A dark brown solution was observed after 168 h, indicating AgNP-K formation.

Characterization of AgNP-K

UV–Visible Spectrophotometer Analysis

Based on Figure 1(A) and 1(B) the UV–vis measurements were performed every 24 h until 168 h and incubated at 60 °C. The peak observed ranged from 400 to 500 nm confirming the reduction of silver ions (Ag^+) to silver (Ag^0) with the sharpest and most intense peak observed at 168th hours of incubation time.

Particle Size and Zeta Potential Measurement

Table 1 summarises the results of the Zetasizer analysis. AgNP-K 1:1 showed an average size distribution of 120.4 nm, while AgNP-K 1:2 was 226.5 nm the polydispersity index (PDI) for AgNP-K 1:1 was 0.462 and AgNP-K 1:2 was 0.315. AgNP-K 1:1 showed a value of -34.1 mV and -33.9 mV for AgNP-K 1:2 for the zeta potential measured.

Transmission Electron Microscope (TEM)

TEM analysis was conducted to observe the surface morphology and size of each AgNP-K by measuring the diameter from the cross-section. From Figure 1(C) and 1(D), it was determined that both the synthesized AgNP-K was nearly spherical. The average diameter size of AgNP-K 1:1 was 16.963 ± 6.0465 nm and AgNP-K 1:2 was 17.083 ± 4.2772 nm. From the TEM images, the particle size distribution was plotted in a histogram as shown in Figure 1(E) and 1(F).

Scanning Electron Microscopy–Energy Dispersive X-RAY Analysis (SEM-EDX)

Scanning electron microscopy–energy dispersive X-ray spectroscopy (SEM-EDX) was used to determine the surface morphology and elemental composition of the synthesized AgNP-K. Based on SEM images in Figure 1(G) and 1(I), both AgNP-K 1:1 and AgNP-K 1:2 had a nearly spherical shape. The EDX spectra graph in Figure 1(H) and 1(J) shows the composition of the AgNP-K. The main components of the measurements were silver and Ag. The results showed that AgNP-K 1:1 had a higher Ag composition, with averages of 61.17% and 35.28% for AgNP-K 1:2, respectively. Whereas C and O peaks were hypothesized to come from the hydrocarbon structure of kaempferol. The unlabeled peaks are unknown, undetected peaks.²²

X-Ray Diffraction Analysis

Figure 2(A) and 2(B) showed the XRD pattern of synthesized AgNP-K. The main peaks for AgNP-K 1:1 clearly appeared at (2θ) 38.19 (111), 44.39 (200), 64.59 (220), 77.58 (311), and 81.74 (222) planes, indicating the face-centred cubic structures of AgNP-K 1:1.^{5,22} Meanwhile, AgNP-K 1:2 showed (2θ) 40.16 (111), 44.40 (200), 64.60 (220), 77.59 (311) and 81.75 (222). The peak was compared with the silver database from the Joint Committee on Powder Diffraction Standard (JCPDS) card no. 9012431 or International Centre for Diffraction Data (ICDD).²² These results showed that

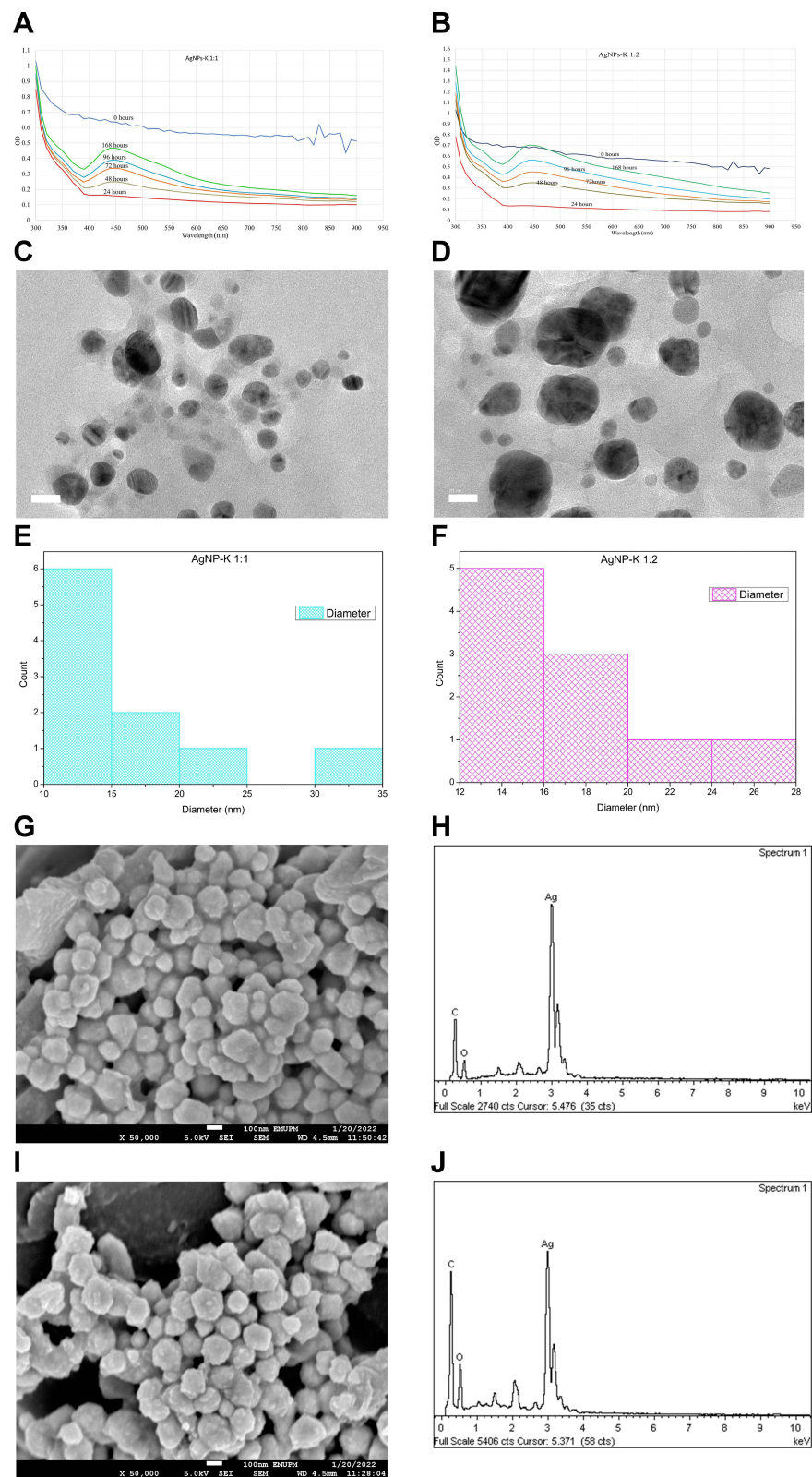


Figure 1 Characterization result from UV-Vis, TEM, and SEM-EDX analysis. **(A)** and **(B)** UV-Vis spectra for AgNP-K 1:1 and AgNP-K 1:2. **(C)** and **(D)** TEM images of AgNP-K 1:1 and AgNP-K 1:2. **(E)** and **(F)** cross-sectional size and diameter measurements of AgNP-K 1:1 and AgNP-K 1:2 presented in histogram graphs. **(G)** and **(H)** SEM-EDX images of AgNP-K 1:1. **(I)** and **(J)** SEM-EDX images of AgNP-K 1:2.

Table 1 Summarized Particle Size, PDI, and Zeta Potential of Both AgNP-K 1:1 and AgNP-K 1:2 Measured by Zetasizer

Sample (Specs)	Size	PDI	Zeta Potential
AgNP-K 1:1 (1 mMol AgNO ₃ :1 mMol K 168h 1 L)	120.4	0.462	-34.1
AgNP-K 1:2 (1 mMol AgNO ₃ :2 mMol K 168h 1 L)	226.5	0.315	-33.9

both AgNP-K (1:1 and 1:2) were pure crystalline and confirmed the presence of silver in the synthesized sample. From the XRD analysis, the crystallite size also could be determined from the formula by Scherrer Equation, $L = K\lambda/\beta \cdot \cos\theta$ whereby XRD radiation of wavelength λ (nm) from measuring full width at half maximum of peaks (β) in radian located at any 2θ in the pattern.²³ The crystallite size for AgNP-K 1:1 was 32.603 nm and AgNP-K 1:2 was 29.5394 nm.

Fourier Transform Infrared Spectrometers (FTIR)

In Figure 2(C), a comparison was made between the blanks (commercial AgNPs and kaempferol) with AgNP-K 1:1 and 1:2. The FTIR spectra of AgNP-K 1:1 showed peaks at 1594.69 cm⁻¹, 1289.58 cm⁻¹, and 801.45 cm⁻¹. Meanwhile, AgNP-K 1:2 showed at 1593.19 cm⁻¹, 1166.68 cm⁻¹. The blank kaempferol exhibited peak at 3145.15 cm⁻¹, 1607.96 cm⁻¹ and 1170.58 cm⁻¹. The peak at 3145.15 cm⁻¹ for blank kaempferol was represented by -OH or -NH groups. This was attributed to the presence of phenolic compounds in kaempferol. Figure 2(D) shows the possible mechanisms of AgNP-K formation.

Antibacterial Activities of AgNP-K Against MRSA

Disc Diffusion Assay (DDA)

Figure 3 shows the zone of inhibition of AgNP-K against MRSA. Table 2 shows the zones of inhibition of MRSA growth after treatment with AgNP-K 1:1 and AgNP-K 1:2. The diameter of inhibition was measured based on the Kirby-Bauer test.¹⁴⁻¹⁶ The biggest zone inhibition of AgNP-K 1:1 and AgNP-K 1:2 against MRSA was 16.67 ± 1.19 mm and 14.43 ± 0.80 mm at 10 mg/mL concentration, respectively. AgNP-K showed greater inhibition of MRSA than kaempferol or commercial AgNPs. The inhibition zones for both samples (AgNP-K 1:1 and AgNP-K 1:2) showed almost similar zones when compared to those of vancomycin. The ANOVA test also showed a significant result ($p < 0.05$) in the inhibition zones of AgNP-K 1:1 and AgNP-K 1:2 when compared with kaempferol and commercial AgNPs.

Minimum Inhibitory Concentration (MIC) and Minimum Bactericidal Concentration (MBC)

The MIC and MBC were carried out to determine the lowest concentration of AgNP-K that prevented the growth of MRSA and the bacteriostatic or bactericidal characteristics of AgNP-K. Bacteriostatic refers to the lowest concentration that inhibits bacterial growth, while bactericidal refers to the lowest concentration that kills the bacteria.²⁴ Table 3 shows the MIC and MBC values of AgNP-K, commercial AgNPs and kaempferol. The MIC of AgNP-K 1:1 against MRSA was 1.25 mg/mL meanwhile the MIC of AgNP-K 1:2 against MRSA was 2.50 mg/mL. The MIC values of both AgNP-K were lower than commercial AgNPs (>10.00 mg/mL) and kaempferol (>10.00 mg/mL). Based on Table 3, AgNP-K 1:1 exhibited the highest antibacterial activity against MRSA compared to other samples. The MBC values of AgNP-K 1:1 and AgNP-K 1:2 against MRSA were 2.50 mg/mL and 5.00 mg/mL, respectively. Whereas the MBC values for the commercial AgNPs and kaempferol were greater than 10 mg/mL (Table 3).

Time-Kill Assay

Time-kill assay was performed to determine the killing rate by time (every 4 hours for 24 hours) of MRSA growth after exposed to AgNP-K 1:1 [(1.25 mg/mL) MIC value] and AgNP-K 1:2 [(2.5 mg/mL) MIC value]. Figure 3(D) shows a graph of the logarithmic number of CFU/mL (log₁₀ CFU/mL) versus time. In this analysis, the growth of the bacteria treated with AgNP-K steadily decreased after 24 h. The growth reduction of MRSA after treatment with AgNP-K 1:1 (1.25 mg/mL) was higher than that after treatment with AgNP-K 1:2 (2.50 mg/mL). The growth reduction of MRSA after being treated with AgNP-K 1:1 and AgNP-K 1:2 for 24 hours were 1.30 log₁₀ CFU/mL and 0.70 log₁₀ CFU/mL, respectively. From the result, there was a significant difference ($p < 0.05$) between MRSA and AgNP-K 1:1 and AgNP-K 1:2.

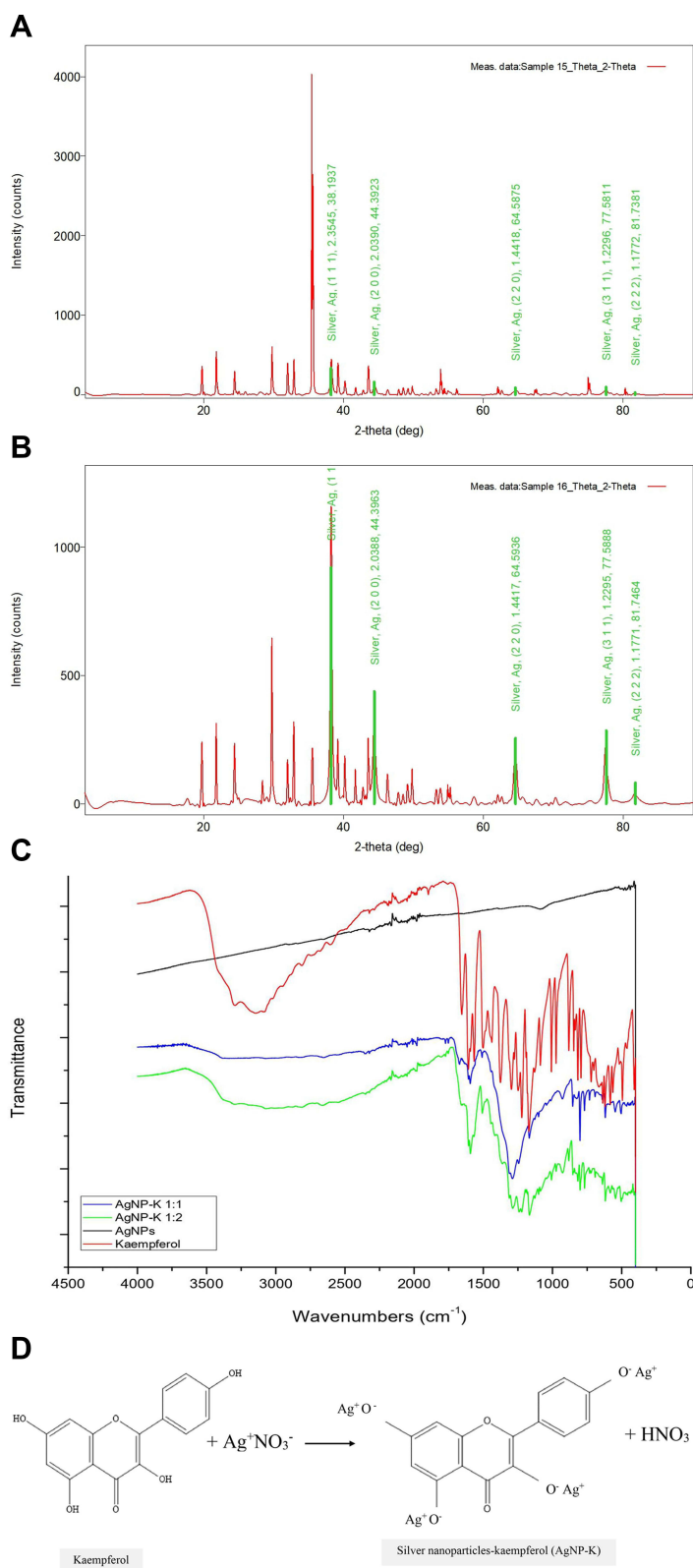


Figure 2 (A) XRD spectra for AgNP-K 1:1 and **(B)** for AgNP-K 1:2. **(C)**: FTIR spectra (AgNP-K 1:1, AgNP-K 1:2, kaempferol and commercial AgNPs). Kaempferol showed a broad peak at around 3500 cm⁻¹ to 3000 cm⁻¹, which is attributed to the hydroxyl (-OH) functional group (H-bond stretching). Another peak at 1386 cm⁻¹ can also be observed, which is attributed to C-H stretching vibration and C-H bending vibration respectively. **(D)**: Possible mechanism of AgNP-K formation based on FTIR results shown in **(C)**: (software: Chemdraw).

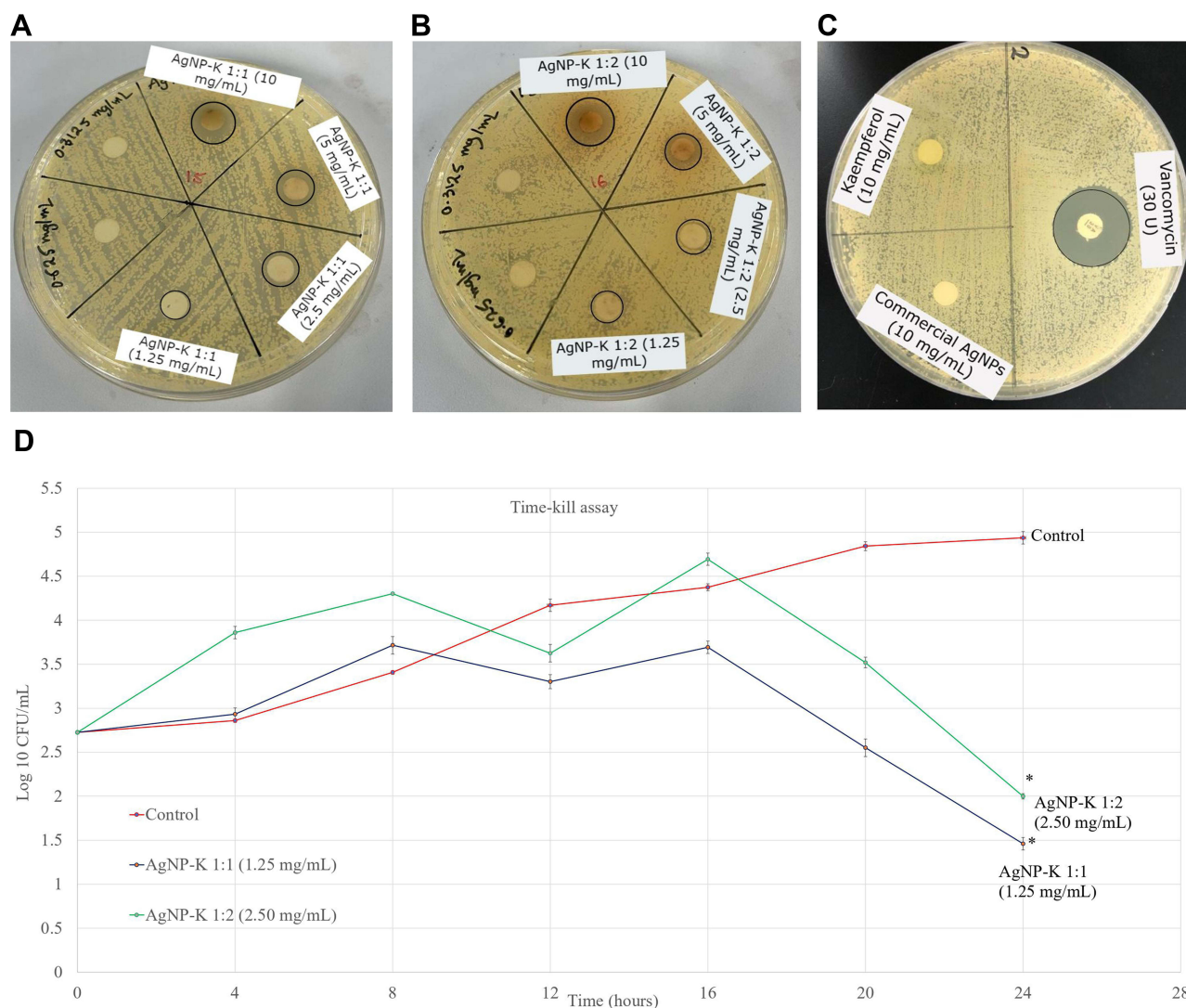


Figure 3 (A) Inhibition zone of AgNP-K 1:1 against MRSA (blue circles). **(B)** Inhibition zone of AgNP-K 1:2 against MRSA (blue circles). **(C)** Inhibition zone of vancomycin (black circle), commercial AgNPs, kaempferol, and sterilized water against MRSA. **(D)** Graph of \log_{10} CFU/mL versus time (measured every 4 hours for 24 hours) for time-kill assay of AgNP-K 1:1 (1.25 mg/mL) and AgNP-K 1:2 (2.50 mg/mL) against MRSA. Values are expressed as mean \pm SD with an asterisk (*) shown statistically significant ($p < 0.05$) from control.

Discussion

Upon the addition of kaempferol to AgNO_3 solution, the sample solution slowly turned brown, indicating the formation of AgNPs due to the reduction of Ag^+ to Ag^0 .^{8,22} An aforementioned study correspondingly described similar findings where the establishment of dark red solution from bright yellow indicated silver nanoparticles formed.²⁵ The green synthesis of AgNPs needs the following requirements: (i) types of solvents used for synthesis, (ii) types of reducing and capping agents, and (iii) non-toxic material used for stabilizing the NPs.²⁶ On this point, kaempferol as a bioactive compound acted as a reducing and capping agent. The synthesis of AgNPs using AgNO_3 as the precursor and water as the dissolving solvent offers high chemical stability and is cost-effective.²⁷ The mechanism of the chemical reaction for the establishment of AgNPs can result from flavonoids and phenolic compounds (reducing and capping agents). These compounds act as electron or hydrogen donors.²⁸ The ketoform on the backbone of a flavonoid compound reduces from Ag^+ to Ag^0 .²⁹ According to previous studies, the optimum temperature to synthesize AgNPs was 60 °C.²² The application of heat (60 °C) helped in the complete reaction of kaempferol with silver.

UV-vis spectroscopy is a crucial method because it was the first checklist to observe the formation of AgNP-K over time. UV-vis spectroscopy was used to observe the surface plasmon resonance (SPR) of the optical properties and electronic

Table 2 The Values of Zone Inhibition of AgNP-K 1:1, AgNP-K 1:2, Kaempferol, Commercial AgNPs, and Vancomycin Against MRSA Measured from DDA Test

Samples	Concentration Samples (mg/mL)			
	Diameter zone (mm)			
	1.25 mg/mL	2.5 mg/mL	5 mg/mL	10 mg/mL
AgNP-K 1:1	8.00 ± 0.82 ^a	8.22 ± 0.31 ^{a,b}	12.44 ± 0.68 ^{b,c}	16.67 ± 1.19 ^c
AgNP-K 1:2	6.00 ± 0.27 ^a	7.56 ± 1.34 ^{a,b}	12.56 ± 1.93 ^{b,c}	14.43 ± 0.80 ^c
Kaempferol (10 mg/mL)	6.00 ± 0.00 ^a			
Commercial AgNPs (10 mg/mL)	6.00 ± 0.00 ^a			
Vancomycin (30 U)	18.00 ± 0.27 ^d			

Notes: Values are represented as mean ± SD. Values in the same row followed by different superscript letters differ significantly ($p < 0.05$) from the control.

Table 3 MIC and MBC Values of AgNP-K 1:1, AgNP-K 1:2, Kaempferol, Commercial AgNPs, and Vancomycin Against MRSA

Samples	MIC (mg/mL)	MBC (mg/mL)
AgNP-K 1:1	1.25	2.50
AgNP-K 1:2	2.50	5.00
Kaempferol (10 mg/mL)	> 10.00	> 10.00
Commercial AgNPs (10 mg/mL)	> 10.00	> 10.00
Vancomycin (10 mg/mL)	< 0.08	< 0.08

structure of the AgNP-K.²² On the surface of the NPs, the electron cloud of the NPs oscillates and electromagnetic waves are absorbed at a particular frequency in the range of 350–500 nm of wavelength.³⁰ AgNP-K 1:1 showed an absorbance peak at 0.47 optical density (OD) of 168 hours meanwhile AgNP-K 1:2 showed 0.70 OD. AgNP-K 1:2 exhibited a higher peak due to the higher concentration (2 mMol) of kaempferol used, leading to a more concentrated sample.

Based on the Zetasizer results, AgNP-K 1:2 shows a larger particle size of 226.5 nm when compared to AgNP-K 1:1 (120.4 nm). These results confirm the Mie-type scattering theory states that the peak location measured from UV–visible light indicates the size of the formed AgNPs.⁵ The theory indicates that a higher concentration of kaempferol results in a larger size of AgNP-K. PDI values for both synthesized AgNP-K 1:1 and AgNP-K 1:2 were in monodisperse phase, referring to the value of PDIs ranging from 0 to 1, whereby 0 was monodisperse and 1 polydisperse. This result corresponds to Mat Yusuf et al study which recorded a PDI value of 0.206 for their synthesized AgNPs using *Clinacanthus nutans*.²² Zeta potential value represents net charges around the NPs, but not the definite surface charges.⁵ The zeta potential values for AgNP-K 1:1 and 1:2 were −34.1 and −33.9, respectively, attributed to charges from phenolic compounds in the bioactive substance. The higher negative values result in a strong repulsive force among particles, preventing their aggregation.^{31,32} Negative charges of AgNP-K will promote the attachment of AgNP-K on the MRSA cell surface by shifting their electrical charges.^{33,34} This, in turn, exhibits AgNP-K properties as an antibacterial agent against MRSA.

The TEM results (Figure 1) showed a different value which was much smaller than the values shown by the Zetasizer. This was due to the previous report stating that the presence of any media during analysis led to the different measurements observed on the particle size.³⁵ Furthermore, Zetasizer measured the hydrodynamic radius in the liquid state meanwhile TEM gave the actual size in a dry state. In addition, TEM was used to analyze the diameter of the cross-section of the AgNP-K; thus, a smaller value was measured. The TEM sizes measured in this study were smaller than those measured by Zetasizer, consistent with previous studies by Mat Yusuf et al Deng et al and Mohamad Hanafiah et al.^{5,8,22} AgNP-K 1:1 was found to be smaller than AgNP-K 1:2 which corresponded to the Zetasizer results. Lower concentrations of kaempferol produced fewer kaempferol molecules, leading to low Ag⁺ ion reduction resulting in smaller AgNP-K formed. This finding is consistent with a study conducted by Deng et al in 2021, where an increase in kaempferol concentration led to an increase in AgNPs size.⁵

SEM-EDX analysis was used to determine the morphology of AgNP-K and its composition, mainly silver (Ag). SEM images of AgNP-K [Figure 1(G) and 1(I)] showed minimal aggregation with a nearly spherical shape. The EDX spectra in Figure 1(H) and 1(J) show the elemental composition (Ag) contained in the synthesized AgNP-K, whereby AgNP-K 1:1 has a higher Ag composition than AgNP-K 1:2. This was due to the binding of biomolecules from kaempferol onto the surface of AgNPs, as well as the high concentration of kaempferol applied to AgNP-K 1:2. This resulted in a lower silver (Ag) composition in the AgNP-K 1:2. This could be due to the higher ratio of kaempferol concentrations used in synthesizing AgNP-K. The higher concentration of kaempferol might reduce the silver composition in AgNP-K and increase the carbon composition, owing to the structural properties of kaempferol itself. This observation was supported by studies conducted by Mat Yusuf et al and Kannanoor et al which showed that a higher concentration of plant extract led to lower silver composition produced.^{22,36}

XRD analysis was conducted to observe the crystallinity of AgNP-K at 2θ angle. The results shown in Figure 2(A) and 2(B) clearly show the peak positions for silver when compared to the silver database from the Joint Committee on Powder Diffraction Standard (JCPDS) or the International Centre for Diffraction Data (ICDD).²² The peak positions between both samples were slightly shifted. This could be attributed to the concentration of kaempferol applied during the synthesis of AgNP-K. The results also confirmed that AgNP-K were pure crystalline or amorphous and could be indexed as a face-centred cubic structure of silver. Crystallite size measured from the XRD graph showed differences compared to particle size measured from TEM and Zetasizer. This difference was assumed, related to experimental error from the Scherrer fitting.³⁷

FTIR analysis was conducted to determine the possible functional groups present in the synthesized AgNP-K. As shown in Figure 2(C) the FTIR spectra of kaempferol showed a broad peak at approximately 3500 cm^{-1} 3000 cm^{-1} , which was ascribed to the hydroxyl (-OH) functional group (H-bond stretching). Another peak at 1386 cm^{-1} can also be detected, which is ascribed to the C-H stretching and C-H bending vibrations. The remaining two peaks at 1590 cm^{-1} and 1022 cm^{-1} also observed can be attributed to C=C stretching vibrations in the aromatic ring. In contrast, the (-OH) groups were not detected in AgNP-K 1:1 and AgNP-K 1:2. The absence of the (-OH) group in AgNP-K 1:1 and AgNP-K 1:2 indicated that kaempferol was successfully incorporated into silver. Based on FTIR analysis, the hydroxyl (-OH) group in phenolic compounds from kaempferol was hypothesized to be responsible for the reduction of Ag^+ to Ag^0 and the stabilization of AgNP-K.^{22,38} These findings were supported by a previous study that stated that phenolic and hydroxyl compounds found in the extracts act as reducing and capping agents, thus stabilizing the AgNP-K formed.^{22,39}

From the DDA analysis, the zone inhibition of MRSA treated with AgNP-K was the largest, while kaempferol and commercial AgNPs showed no inhibition. This proved the synergistic effect when AgNPs were incorporated with kaempferol. AgNPs synthesized with plant extracts exhibited strong antimicrobial activity and the inhibitory capability remained dependent on the AgNPs concentration. The antimicrobial susceptibility of Gram-positive and Gram-negative bacteria depends on the structural characteristics of the studied species, shape, size of the NPs, and exposure time.⁴⁰ This could be attributed to the smaller size of AgNP-K and the silver composition of the compound itself. The size of AgNPs was also found to play a significant role in reducing microbial growth. Smaller NPs facilitated the penetration of NPs into the bacterial membrane.^{8,41–44} AgNPs allow other molecules, such as antibiotics, to penetrate the bacteria by increasing the membrane permeability of the bacterial cell wall, thus turning an inefficient drug into an efficient substitute treatment possibility.⁴⁰ This leads to the fully maximized capability of AgNP-K.

MIC and MBC analyses demonstrated that AgNP-K 1:1 had a superior inhibitory effect on MRSA compared to AgNP-K 1:2. The bacteriostatic and bactericidal activities of a drug can be determined using the MIC and MBC values. Bactericidal activity was defined as an MBC value that is less than 4x of the MIC values. Whereas bacteriostatic status was defined as an MBC of more than 4x MIC values. Based on Table 3, the MIC value for AgNP-K 1:1 was 1.25 mg/mL, while the MBC value was 2.5 mg/mL (2x MIC value). On the other hand, AgNP-K 1:2 MIC value was 2.5 mg/mL, and its MBC value was 5.0 mg/mL (2x MIC value).¹⁸ From MIC and MBC analyses, both AgNP-K 1:1 and AgNP-K 1:2 exhibited bactericidal agents against MRSA.

Time-kill assay was performed to determine the killing rate by time (every 4 hours for 24 hours) of MRSA growth after exposed to AgNP-K 1:1 [(1.25 mg/mL) MIC value] and AgNP-K 1:2 [(2.5 mg/mL) MIC value]. Bactericidal activity was achieved when the treatment reduced more than $>3\log_{10}$ CFU/mL colony-forming units (CFU) from the initial inoculum by $>3\log_{10}$ CFU/mL. Meanwhile, bacteriostatic activity was achieved when antibacterial agents reduced less than $<3\log_{10}$ CFU/

mL from the initial inoculum.²⁰ From the time-kill assay, AgNP-K 1:1 and AgNP-K 1:2 acted as bacteriostatic agents towards MRSA because both samples were reduced less than \log_{10} CFU/mL of MRSA growth from the initial state ($p < 0.05$).

Conclusion

A successful green synthesis of silver nanoparticles combined with kaempferol (AgNP-K) has been achieved, demonstrating substantial antibacterial effectiveness against MRSA. This method offers numerous benefits, including its simplicity, as it only requires two reagents (silver nitrate and kaempferol) and does not involve the use of any extra chemicals, making it an environmentally friendly approach. In a biological assessment, AgNP-K displayed outstanding antibacterial performance against MRSA when compared to both commercially available AgNPs and kaempferol. The synergistic activity exhibited by AgNP-K possesses tremendous potential to be developed as an alternative treatment against MRSA.

Acknowledgments

The authors acknowledge Universiti Sains Islam Malaysia and Universiti Putra Malaysia (UPM) for providing laboratory accommodations.

Funding

This study was funded by the Ministry of Higher Education (MOHE) under Fundamental Research Grant Scheme, (FRGS) Code: (FRGS/1/2020/STG05/USIM/02/2).

Disclosure

The authors report no conflicts of interest in this work.

References

- Lakhundi S, Zhang K. Methicillin-resistant *Staphylococcus aureus*: molecular characterization, evolution, and epidemiology. *Clin Microbiol Rev*. 2018;31(4):e00020–18. doi:10.1128/CMR.00020-18
- Adnan SN, Ibrahim N, Yaacob WA. Disruption of Methicillin-resistant *Staphylococcus aureus* protein synthesis by tannins. *Germs*. 2017;7(4):186. doi:10.18683/germs.2017.1125
- Stapleton PD, Taylor PW. Methicillin resistance in *Staphylococcus aureus*: mechanisms and modulation. *Sci Prog*. 2002;85(1):57–72. doi:10.3184/003685002783238870
- Nataraj BH, Mallappa RH. Antibiotic resistance crisis: an update on antagonistic interactions between probiotics and methicillin-resistant staphylococcus aureus (MRSA). *Currentmicrobio*. 2021;78(6):2194–2211.
- Deng SP, Zhang JY, Ma ZW, Wen S, Tan S, Cai JY. Facile synthesis of long-term stable silver nanoparticles by kaempferol and their enhanced antibacterial activity against *Escherichia coli* and *Staphylococcus aureus*. *J Inorg Organomet Polym Mater*. 2021;31(7):2766–2778.
- Devi KP, Malar DS, Nabavi SF, et al. Kaempferol and inflammation: from chemistry to medicine. *Pharmacol Res*. 2015; 2015(99):1–10.
- Hanafiah RM, Aqma WS, Yaacob WA, Said Z, Ibrahim N. Antibacterial and biofilm inhibition activities of *Melastoma malabathricum* stem bark extract against *Streptococcus mutans*. *Malays j microbio*. 2015;2015:1.
- Mohamad Hanafiah R, Abd Ghafar SA, Lim V, Musa SNA, Yakop F, Hairil Anuar AH. Green synthesis, characterisation and antibacterial activities of strobilanthes crispus-mediated silver nanoparticles (SC-AGNPS) against selected bacteria. *Artif Cells Nanomed Biotechnol*. 2023;51(1):549–559.
- Sampath G, Govarthanan M, Rameshkumar N, et al. Eco-friendly biosynthesis metallic silver nanoparticles using Aegle marmelos (Indian bael) and its clinical and environmental applications. *Appl Nanosci*. 2023;13(1):663–674.
- Valarmathi N, Ameen F, Almansob A, Kumar P, Arunprakash S, Govarthanan M. Utilization of marine seaweed *Spyridia filamentosa* for silver nanoparticles synthesis and its clinical applications. *Mater Lett*. 2020;263:127244. doi:10.1016/j.matlet.2019.127244
- Ameen F, Srinivasan P, Selvankumar T, et al. Phytosynthesis of silver nanoparticles using *Mangifera indica* flower extract as bioreductant and their broad-spectrum antibacterial activity. *Bioorg Chem*. 2019;88(102970):102970. doi:10.1016/j.bioorg.2019.102970
- Mythili R, Selvankumar T, Kamala-Kannan S, et al. Utilization of market vegetable waste for silver nanoparticle synthesis and its antibacterial activity. *Mater Lett*. 2018;225:101–104. doi:10.1016/j.matlet.2018.04.111
- Govarthanan M, Seo YS, Lee KJ, et al. Low-cost and eco-friendly synthesis of silver nanoparticles using coconut (*Cocos nucifera*) oil cake extract and its antibacterial activity. *Artif Cells Nanomed Biotechnol*. 2016;44(8):1878–1882. doi:10.3109/21691401.2015.1111230
- Yakop F, Abd Ghafar SA, Yong YK, et al. Silver nanoparticles *Clinacanthus Nutans* leaves extract induced apoptosis towards oral squamous cell carcinoma cell lines. *Artif Cells Nanomed Biotechnol*. 2018;46(sup2):131–139. doi:10.1080/21691401.2018.1452750
- Drew WL, Barry AL, O'Toole R, Sherris JC. Reliability of the Kirby-Bauer disc diffusion method for detecting methicillin-resistant strains of staphylococcus aureus. *Appl Microbiol*. 1972;24(2):240–247. doi:10.1128/am.24.2.240-247.1972
- Hudzicki J. Kirby-Bauer disk diffusion susceptibility test protocol. *Am Soc Microbiol*. 2009;15:55–63.
- Cong Y, Yang S, Rao X. Vancomycin resistant *Staphylococcus aureus* infections: a review of case updating and clinical features. *J Adv Res*. 2020;21:169–176. doi:10.1016/j.jare.2019.10.005
- Hanafiah RM, Kamaruddin KAC, Saikin NAA, et al. Antibacterial properties of *clinacanthus nutans* extracts against *porphyromonas gingivalis* and aggregatibacter actinomycetemcomitans: an in-vitro study. *J Int Dent Medical Res*. 2019;19:1

19. Giuliano C, Patel CR, Kale-Pradhan PB. A guide to bacterial culture identification and results interpretation. *Pharm Ther.* **2019**;44(4):192. doi:10.1017/ice.2016.82
20. Abd Ghafar SA, Salehuddin NS, Abdul Rahman NZ, Halib N, Mohamad Hanafiah R. Transcriptomic profile analysis of *Streptococcus mutans* response to *Acmella paniculata* flower extracts. *Evid Based Complement Alternat Med.* **2022**;2022:1–14. doi:10.1155/2022/7767940
21. Rani R, Sharma D, Chaturvedi M, Yadav JP. Antibacterial activity of twenty different endophytic fungi isolated from *Calotropis procera* and time-kill assay. *Clin Microbiol.* **2017**;6(3):280. doi:10.4172/2327-5073.1000280
22. Mat Yusuf SNA, Che Mood CNA, Ahmad NH, Sandai D, Lee CK, Lim V. Optimization of biogenic synthesis of silver nanoparticles from flavonoid-rich *Clinacanthus nutans* leaf and stem aqueous extracts. *Royal Soc Open Sci.* **2020**;7(7):200065. doi:10.1098/rsos.200065
23. Monshi A, Foroughi MR, Monshi MR. Modified Scherrer equation to estimate more accurately nano-crystallite size using XRD. *World J Nano Sci Eng.* **2012**;2(3):154–160. doi:10.4236/wjnse.2012.23020
24. Shami AY, Almasri RA. Research article bacteriostatic and bactericidal activity of deer musk on multidrug resistance bacteria. *Pak. J Biol Sci.* **2018**;21:331–339.
25. González AL, Noguez C. Size, shape, stability, and color of plasmonic silver nanoparticles. *J Phys Chem.* **2014**;118(17):9128–9136. doi:10.1021/jp5014434
26. Raveendran P, Fu J, Wallen SLJAVKS. Silver nanoparticles: green synthesis and their antimicrobial activities. *Chem Soc.* **2003**;125(46):13940. doi:10.1021/ja029267j
27. Vijayaraghavan K, Nalini SK. Biotemplates in the green synthesis of silver nanoparticles. *Biotechnol J.* **2010**;5(10):1098–1110. doi:10.1002/biot.201000167
28. Pietta PG. Flavonoids as antioxidants. *J Natural Prod.* **2000**;63(7):1035–1042. doi:10.1021/np9904509
29. Ambika S, Sundrarajan M. Antibacterial behaviour of Vitex negundo extract assisted ZnO nanoparticles against pathogenic bacteria. *J Photochem Photobiol B Biol.* **2015**;146:52–57. doi:10.1016/j.jphotobiol.2015.02.020
30. Abdelhalim MAK, Mady MM. Physical properties of different gold nanoparticles: ultraviolet-visible and fluorescence measurements. *J Nanomed Nanotechnol.* **2012**;3(3):178–194. doi:10.4172/2157-7439.1000133
31. Ghorbani HR, Safekordi AA, Attar H, Sorkhabadi SM. Biological and non-biological methods for silver nanoparticles synthesis. *Chem Biochem Eng Q.* **2011**;25(3):317–326.
32. Priyadarshini S, Gopinath V, Priyadarshini NM, MubarakAli D, Velusamy P. Synthesis of anisotropic silver nanoparticles using novel strain, *Bacillus flexus* and its biomedical application. *Colloids Surf.* **2013**;102:232–237. doi:10.1016/j.colsurfb.2012.08.018
33. Qing YA, Cheng L, Li R, et al. Potential antibacterial mechanism of silver nanoparticles and the optimization of orthopedic implants by advanced modification. *Int J Nanomed.* **2018**;13:3311–3327. doi:10.2147/IJN.S165125
34. More PR, Pandit S, Filippis AD, Franci G, Mijakovic I, Galdiero M. Silver nanoparticles: bactericidal and mechanistic approach against drug resistant pathogens. *Microorganisms.* **2023**;11(2):369. doi:10.3390/microorganisms11020369
35. Chartarrayawadee W, Charoensin P, Saenma J, et al. Green synthesis and stabilization of silver nanoparticles using *Lysimachia foenum-graecum* Hance extract and their antibacterial activity. *Green Process Synth.* **2020**;9(1):107–118. doi:10.1515/gps-2020-0012
36. Kannanoor M, Lakshmi BA, Kim S. Synthesis of silver nanoparticles conjugated with kaempferol and hydrocortisone and an evaluation of their antibacterial effects. *Biotechnol Prog.* **2021**;11(7):317.
37. Schmidt R. (2014). Re: why is there a difference in the crystalline size of the nanoparticle as measured from TEM image and XRD analysis of the same sample?; Available from: <https://www.researchgate.net/post/Why-is-there-a-difference-in-the-crystalline-size-of-the-nanoparticle-as-measured-from-TEM-image-and-XRD-analysis-of-the-same-sample/535b9d33d3df3e84118b4674/citation/download>. Accessed January 30, 2024.
38. Vivek R, Thangam R, Muthuchelian K, Gunasekaran P, Kaveri K, Kannan S. Green biosynthesis of silver nanoparticles from *Annona squamosa* leaf extract and its in vitro cytotoxic effect on MCF-7 cells. *Process Biochem.* **2012**;47(12):2405–2410.
39. Al-Zahrani S, Astudillo-Calderón S, Pintos B, et al. Role of synthetic plant extracts on the production of silver-derived nanoparticles. *Plants.* **2021**;10(8):1671. doi:10.3390/plants10081671
40. Tanase C, Berta L, Mare A, et al. Biosynthesis of silver nanoparticles using aqueous bark extract of *Picea abies* L and their antibacterial activity. *Eur J Wood Prod.* **2020**;78(2):281–291.
41. Potbhare AK, Umekar MS, Chouke PB, et al. Bioinspired graphene-based silver nanoparticles: fabrication, characterization and antibacterial activity. *Mater Today Proc.* **2020**;29:720–725.
42. Potbhare AK, Chaudhary RG, Chouke PB, et al. Phytosynthesis of nearly monodisperse CuO nanospheres using *Phyllanthus reticulatus*/Conyza bonariensis and its antioxidant/antibacterial assays. *Mater Sci Eng C.* **2019**;99:783–793. doi:10.1016/j.msec.2019.02.010
43. Chaudhary RG, Bhusari GS, Tiple AD, et al. Metal/metal oxide nanoparticles: toxicity, applications, and future prospects. *Curr Pharm Des.* **2019**;25(37):4013–4029.
44. Golabiazar R, Othman KI, Khalid KM, Maruf DH, Aulla SM, Yusif PA. Green synthesis, characterization, and investigation antibacterial activity of silver nanoparticles using *Pistacia atlantica* leaf extract. *Bionanoscience.* **2019**;9(2):323–333.

International Journal of Nanomedicine

Dovepress

Publish your work in this journal

The International Journal of Nanomedicine is an international, peer-reviewed journal focusing on the application of nanotechnology in diagnostics, therapeutics, and drug delivery systems throughout the biomedical field. This journal is indexed on PubMed Central, MedLine, CAS, SciSearch®, Current Contents®/Clinical Medicine, Journal Citation Reports/Science Edition, EMBASE, Scopus and the Elsevier Bibliographic databases. The manuscript management system is completely online and includes a very quick and fair peer-review system, which is all easy to use. Visit <http://www.dovepress.com/testimonials.php> to read real quotes from published authors.

Submit your manuscript here: <https://www.dovepress.com/international-journal-of-nanomedicine-journal>